

# Tuning of the Morphology of Core–Shell–Corona Micelles in Water. I. Transition from Sphere to Cylinder

Liangcai Lei,<sup>†,§</sup> Jean-François Gohy,<sup>†</sup> Nicolas Willet,<sup>†</sup> Jian-Xin Zhang,<sup>‡</sup> Sunil Varshney,<sup>‡</sup> and Robert Jérôme<sup>\*,†</sup>

Centre for Education and Research on Macromolecules (CERM), Institute of Chemistry B6, University of Liège, Sart-Tilman, B-4000 Liège, Belgium, and Polymer Source, 771 Lajoie Street, Dorval, Québec, H9P 1G7 Canada

Received February 27, 2003; Revised Manuscript Received November 18, 2003

**ABSTRACT:** Poly(styrene)-*block*-poly(2-vinylpyridine)-*block*-poly(ethylene oxide) (PS-*b*-P2VP-*b*-PEO) ABC triblock copolymers commonly form core–shell–corona (CSC) micelles in water. These micelles consist of a PS spherical core, a P2VP shell, and a PEO corona. However, when the micelles are formed in the presence of a solvent selective for the PS block (benzene), the micellar morphology exhibits a sphere-to-rod transition, as result of the increased volume fraction of the core-forming blocks. Transmission electron microscopy (TEM) and atomic force microscopy (AFM) confirm that a PS rod-like core is surrounded by a P2VP shell and an external PEO corona. Nevertheless, the rod-like micelles coexist with spherical micelles that should be thermodynamically less stable, because of a higher stretching of the PS chains in the core. The P2VP chains are also in a stretched conformation, whatever the pH. The P2VP shell has been used as nanoreactor for the production of gold nanoparticles.

## Introduction

Amphiphilic block copolymers dissolved in a solvent selective for one block exhibit a complex self-assembling behavior.<sup>1</sup> Formation of nanostructures in synthetic polymers is a stimulating challenge in order to meet the requirements for quite different applications, for example, preparation of nanoobjects,<sup>2</sup> membrane reconstruction,<sup>3</sup> and imitation of life systems.<sup>4</sup> A large variety of diblock copolymers have been studied extensively in the past two decades and much information has been collected.<sup>1</sup> Quite interestingly, size and shape of block copolymer self-assemblies may be sensitive to external stimuli, such as concentration, solvent, pH, and temperature.<sup>5</sup> Although ABC triblocks are known for a larger variety of phase separated structures in the bulk compared to diblocks,<sup>6</sup> little is known about their associative behavior in solution. Formation of “three-layer” micelles was first reported for an ABC triblock copolymer in a selective solvent,<sup>7</sup> similarly to the coprecipitation of a mixture of two diblocks.<sup>8</sup> Recently, asymmetric “Janus” micelles were prepared, consisting of a cross-linked poly(butadiene) core and a corona with a “southern” poly(styrene) and a “northern” poly(methyl methacrylate) hemisphere.<sup>9</sup> These “Janus” micelles were shown to form super-aggregates whenever a nonsolvent of one of the coronal hemispheres was used. Temperature- and pH-sensitive core–shell–corona (CSC) micelles, whose shell is selectively cross-linkable, were also reported quite recently.<sup>10</sup> Some of us reported on the formation of pH-sensitive core–shell–corona spherical micelles with a PS core, a P2VP shell, and a PEO corona by an ABC polystyrene-*block*-poly(2-vinylpyridine)-*block*-poly(ethylene oxide) copolymer (PS-*b*-P2VP-*b*-PEO) in water.<sup>11</sup> Moreover, the shell of these micelles responds

reversibly to a change in the environmental pH, due to the (de)protonation of the P2VP blocks.<sup>12</sup>

Although spherical micelles are generally formed by diblock copolymers, other morphologies including rods, tubules, and vesicles can be generated, as exemplified by “crew-cut” micelles<sup>13</sup> and “rod-coil” copolymers.<sup>14</sup> These nonspherical morphologies are now actively studied, because of potential application in nanoscience. The morphology of micelles or aggregates is mainly governed by three contributions to the free energy of micellization, i.e., the stretching entropy of the core-forming blocks, the repulsive interaction of the coronal chains and, for diblock copolymers, the interfacial energy at the core–corona interface.<sup>15</sup> There are different ways of tuning these contributions and, in turn, for designing the morphology of the micelles or aggregates. For instance, the core-forming blocks are expected to be stretched, and the energy of the core–corona interface to be modified by the addition of a selective solvent for these blocks to the micellization medium.<sup>16</sup> A morphological transition from spheres to rods or other morphologies might be accordingly expected.

This paper aims at reporting on rod-like micelles with a core–shell–corona substructure formed by PS-*b*-P2VP-*b*-PEO copolymers in water. The complexing properties of the P2VP shell, e.g., toward metallic salts, make it an interesting nanoreactor for the preparation of metallic nanoparticles.<sup>11</sup>

## Experimental Section

**Materials.** PS-*b*-P2VP-*b*-PEO copolymers were synthesized by sequential anionic polymerization of the comonomers, as reported elsewhere.<sup>12</sup> The molecular characteristics of the two triblock copolymers used in this study are listed in Table 1.

**Preparation of the Micelles.** A 0.02 g quantity of PS-*b*-P2VP-*b*-PEO was dissolved into 0.9 g of *N,N*-dimethylformamide-benzene (toluene) mixtures of various compositions, i.e., 50, 30, 20, 10, 7, and 4 wt % of benzene (toluene). Water (0.1 g) was then added dropwise to the solution under vigorous stirring, which was maintained for 5 h, and 24 h in some cases. No substantial difference was observed for samples prepared

\* To whom correspondence should be addressed.

<sup>†</sup> CERM, University of Liège.

<sup>‡</sup> Polymer Source.

<sup>§</sup> Permanent address: Department of Applied Chemistry, Liaoning University of Petroleum and Chemical Technology, Fushun, P. R. China.

**Table 1. Molecular Characteristics of the Investigated ABC Triblock Copolymers**

	$M_n$ (PS)	$M_w/M_n$ (PS)	$M_n$ (P2VP)	$M_w/M_n$ (PS- <i>b</i> -P2VP)	$M_n$ (PEO)	$M_w/M_n$ (PS- <i>b</i> -P2VP- <i>b</i> -PEO)
PS <sub>200</sub> - <i>b</i> -P2VP <sub>140</sub> - <i>b</i> -PEO <sub>590</sub>	20 000	1.05	14 000	1.05	26 000	1.1
PS <sub>140</sub> - <i>b</i> -P2VP <sub>120</sub> - <i>b</i> -PEO <sub>795</sub>	14 000	1.05	12 000	1.05	35 000	1.1

**Table 2. Shape and Size of the CSC Micelles Prepared at pH > 5**

organic solvent	copolymer	morphology	$D_{CS}^a$	$D_C^a$	$H_S^a$	$H_{Co}^a$	$S_{PS}^c$
DMF–benzene (70 wt % DMF)	PS <sub>200</sub> –P2VP <sub>140</sub> –PEO <sub>590</sub>	cylinder	58	28	15	20	1.5
		sphere	73	41	16	20	2.2
	PS <sub>140</sub> –P2VP <sub>120</sub> –PEO <sub>795</sub>	cylinder	48	26	11		1.7
		sphere	62	36	13		2.3
DMF <sup>b</sup>	PS <sub>200</sub> –P2VP <sub>140</sub> –PEO <sub>590</sub>	sphere	35	20	7.5		1.1
	PS <sub>140</sub> –P2VP <sub>120</sub> –PEO <sub>795</sub>	sphere	25	14	5.5		0.9

<sup>a</sup>  $D_{CS}$ ,  $D_C$ ,  $H_S$ , and  $H_{Co}$  were extracted from TEM pictures (nm,  $H_{Co}$  is the thickness of the PEO corona). <sup>b</sup> Data for micelles prepared from pure DMF. <sup>12</sup> <sup>c</sup> Stretching of the PS blocks ( $S_{PS}$ ) was estimated as the ratio of the core radius to the unperturbed end-to-end distance of PS.

from benzene or toluene. After “freezing” the micelles with 1 mL of water, the organic solvent was dialyzed against water for 5 days. Micelles were protonated by stirring the micelles in a 0.1 M HCl solution for 24 h.

**Gold-Loaded Nanotubes.** Gold nanotubes were prepared by loading the aqueous micellar solution by an excess of H<sub>2</sub>AuCl<sub>4</sub> under stirring for 4 days. The unreacted H<sub>2</sub>AuCl<sub>4</sub> was then eliminated by dialysis against acidic water. The gold-containing anion was reduced by either electron irradiation during TEM observation or by chemical reaction. The chemical reduction was carried out by adding an excess of an aqueous solution of either NaBH<sub>4</sub> or hydrazine, as described elsewhere.<sup>17</sup> The excess of reducer was removed by dialysis.

**Transmission Electron Microscopy (TEM).** TEM images were recorded with a Philips CM100 microscope equipped with a Gatan 673 CCD camera and transferred to a computer equipped with the Kontron KS100 system. Samples were prepared by dipping a Formvar-coated copper grid into a dilute micellar solution (0.05 wt % polymer), and contrasted with RuO<sub>4</sub> vapor. Samples were also stained by H<sub>3</sub>PO<sub>4</sub>·12WO<sub>4</sub>, by depositing a drop of 0.1 wt % phosphotungstic acid aqueous solution onto the surface of the sample-loaded grid. Three minutes later the solution was blotted with a filter paper, and the sample was then washed with water and dried in air. The standard deviation for the characteristic sizes measured by TEM was 2 nm for all the micrographs.

**Atomic Force Microscopy (AFM).** AFM was carried out with a Multimode Nanoscope IIIa microscope from Digital Instruments Inc. The tapping mode provided height and phase cartography simultaneously. The AFM experiments were carried out directly on the TEM grid (cf. supra). These grids were glued with a double-sided rubber tape on a metal disk magnetically attached to the piezo tube of the microscope. The error on the AFM measurements was roughly estimated at 5 nm.

**Scanning Electron Microscopy (SEM).** SEM was performed with a JEOL JSM-840 A microscope. The micelles were deposited on a silicon wafer, dried, and coated with platinum (sputtering with Balzers SCP-20 for 120 s under argon atmosphere). The standard deviation for the characteristic sizes measured by SEM was 2 nm.

**Dynamic Light Scattering (DLS).** DLS measurements were performed with a Brookhaven Instruments Corp. BI-200 apparatus equipped with a BI-2030 digital correlator and an Ion Laser Technology argon laser with a wavelength of 488 nm and a scattering angle of 90°. A refractive index matching bath of filtered water surrounded the scattering cell, and the temperature was controlled at 25 °C. The scattered intensity was measured as a function of the amount of water added to trigger micellization.

## Results and Discussion

This study aims at changing the morphology of PS-*b*-P2VP-*b*-PEO core–shell–corona (CSC) micelles by the

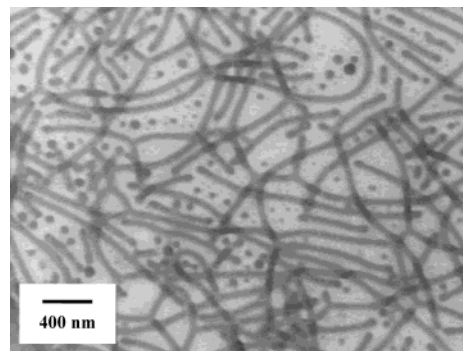


**Figure 1.** TEM micrograph of PS<sub>200</sub>–P2VP<sub>140</sub>–*b*-PEO<sub>590</sub> micelles (rods and spheres) prepared from a 75/25 wt/wt DMF–benzene mixture and contrasted with RuO<sub>4</sub>.

addition of a solvent selective for the PS block (benzene or toluene). The original micelles consist of a PS core, a P2VP corona, and a PEO shell, as shown later. The CSC micelles were prepared by the dropwise addition of water to a copolymer solution in a mixture of a nonselective solvent (DMF) and benzene (toluene). A critical amount of water is required for initiating the copolymer self-assembly. Finally, DMF was dialyzed against water, and the micelles were recovered in pure water. They are extremely stable, being kinetically “frozen” in by the formation of a high  $T_g$  PS core, as previously reported.<sup>13</sup> Because this preparation method is based on the temporary use of a ternary solvent mixture, the micellization mechanism must be complex, as discussed hereafter. The reproducibility of this micellization technique must be pointed out, as must the change in the micellar characteristic features by the addition of benzene (toluene), as well. Because the observations are independent of the solvent selective for PS (benzene or toluene), benzene has been used in a systematic way.

Spherical micelles are collected whenever micellization of the two triblocks under consideration is carried out in DMF/water mixtures followed by dialysis. The characteristic features of the micelles are listed in Table 2. Addition of a selective solvent for the core-forming block has a dramatic impact on the micellar morphology, as shown in Figure 1. Indeed, cylindrical micelles are formed in addition to spherical micelles, in strong dependence on the benzene content. Only spherical micelles are observed when the benzene content in the DMF/benzene mixture is lower than 5 wt %. Their size is quite comparable to that of one of the micelles prepared from pure DMF.<sup>11,12</sup> A mixture of cylindrical and larger

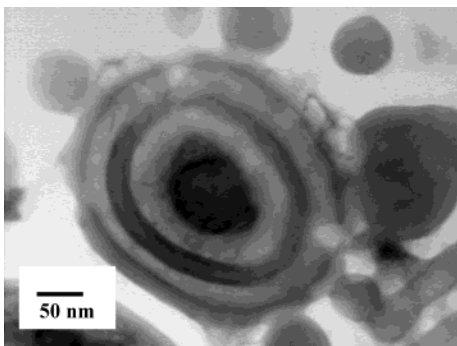


**Figure 2.** TEM micrograph of  $\text{PS}_{200}\text{-}b\text{-P2VP}_{140}\text{-}b\text{-PEO}_{590}$  micelles (onions) prepared from a 70/30 wt/wt DMF–benzene mixture and contrasted with  $\text{RuO}_4$ .

spherical micelles appears when the benzene content exceeds 5 wt %. The relative importance of the cylindrical micelles increases with the benzene content, and this morphology is predominant in the range of 20–35 wt % of benzene, as shown in Figure 1. An onion-like vesicular morphology is, however, formed at benzene content higher than 30 wt % (Figure 2). Whenever the benzene content is larger than 70 wt %, only a few rods persist and onions dominate. These morphologies have been observed after dialysis and are thus “frozen” in pure water.

The onion morphology seems to be an unstable transient structure, as confirmed by the change in the sample morphology during dialysis. In this respect, TEM pictures for samples withdrawn from the dialysis bag show that a mixture of spherical, rod-like and onion-like micelles is formed initially in the presence of 30 wt % of benzene. The number and size of the onions decrease with the progress of dialysis, whereas the characteristic size of the cylinders and spheres remains constant. After 3 days, onions are no longer observed, and the structure of spheres and rods remains unchanged even for long dialysis times (70 days), which is evidence for the “freezing-in” of the final micelles in pure water.

The PS core and P2VP shell of the micelles shown in Figure 1 have been selectively stained by  $\text{RuO}_4$ , with the purpose to measure the diameter of the core+shell ( $D_{\text{CS}}$ ) micellar substructure, for both the rod-like and spherical micelles. These data are reported in Table 2. The cylindrical micelles have the same  $D_{\text{CS}}$  (58 nm for the  $\text{PS}_{200}\text{-}b\text{-P2VP}_{140}\text{-}b\text{-PEO}_{590}$  triblock), whatever the amount of benzene in the initial mixture (in the 7–50 wt % range). In contrast, the length is highly variable, and branched structures are sometimes observed as shown in Figure 3. The mean  $D_{\text{CS}}$  for the spherical micelles is 73 nm, thus larger than  $D_{\text{CS}}$  for the cylinders and for the spherical micelles formed in the absence of benzene (Table 2).  $D_{\text{CS}}$  for the rod-like micelles of the  $\text{PS}_{140}\text{-}b\text{-P2VP}_{120}\text{-}b\text{-PEO}_{795}$  copolymer is 48 nm, compared to 62 nm for the spherical micelles. The P2VP shell of the CSC micelles can be selectively contrasted by  $\text{H}_3\text{PO}_4\cdot 12\text{WO}_4$  as shown elsewhere and as illustrated in Figures 4a and 4b for the  $\text{PS}_{200}\text{-}b\text{-P2VP}_{140}\text{-}b\text{-PEO}_{590}$  sample and in Figure 5 for the  $\text{PS}_{140}\text{-}b\text{-P2VP}_{120}\text{-}b\text{-PEO}_{795}$  micelles. This selectivity allows the thickness of the P2VP shell ( $H_s$ ) and the diameter of the PS core ( $D_c$ ) to be determined. These experimental data, listed in Table 2, show a correlation between the average degree of polymerization of the PS and the P2VP blocks and  $D_c$  and  $H_s$ , respectively. Because spherical and rod-

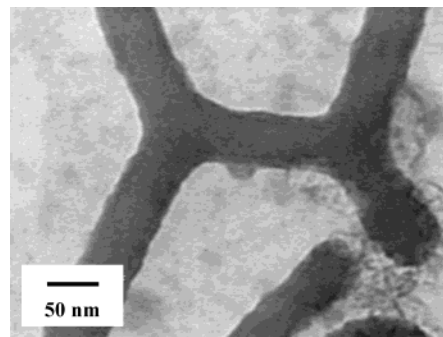


**Figure 3.** TEM micrograph of  $\text{PS}_{200}\text{-}b\text{-P2VP}_{140}\text{-}b\text{-PEO}_{590}$  micelles (branched rods) prepared from a 70/30 wt/wt DMF–benzene mixture and contrasted with  $\text{RuO}_4$ .

like micelles coexist in solution, their hydrodynamic diameter cannot be measured accurately. Nevertheless, the whole diameter ( $D_{\text{CSC}}$ ) of the rod-like and spherical micelles was measured in the dried state by three independent techniques. After exposure of the samples to  $\text{RuO}_4$  vapor for a long time, TEM pictures (Figure 4c) show spherical and rod-like micelles. The underlying Formvar film appears to be stained, in contrast to the PEO corona which is unaffected. Nonaggregated chains adsorbed on the Formvar film could contribute to this “negative” contrast. This unique combination of “negative” contrast of the substrate and “positive” contrast of the core and shell of the micelles allows the thickness of the PEO corona to be measured. A thickness of 20 nm is found for the spherical and rod-like micelles of  $\text{PS}_{200}\text{-}b\text{-P2VP}_{140}\text{-}b\text{-PEO}_{590}$ . The grids observed by TEM were also examined by AFM. This procedure allows to preclude any interference of the sample preparation on the shape and size of the micelles measured by the two techniques. The topography images for spherical and rod-like micelles of  $\text{PS}_{200}\text{-}b\text{-P2VP}_{140}\text{-}b\text{-PEO}_{590}$  are shown in Figure 4d. The whole diameter of the dried cylinders ( $D_{\text{CSC}}$ ) was measured and found to be ca. 90 nm, whereas  $D_{\text{CSC}}$  for the spherical micelles was approximated to 110 nm, which is in good agreement with TEM observations. Therefore, tip-convolution effects are limited in this case. Finally, the same sample was metallized with platinum and observed by SEM (Figure 6).  $D_{\text{CSC}}$  for rod-like and spherical micelles are then 90 and 105 nm, respectively, consistent with the data collected by the two previous methods. Combination of all the experimental data provides a complete description of the micellar substructure, including the size of each compartment.

We previously showed that the shell of  $\text{PS-}b\text{-P2VP-}b\text{-PEO}$  spherical micelles was pH-responsive.<sup>11,12</sup> At  $\text{pH} > 5$ , the P2VP shell is neutral, hydrophobic, and collapsed on the PS core. In contrast, at  $\text{pH} < 5$ , the P2VP shell is protonated, water soluble, with an extended conformation. The reversible switching between the two states was shown by dynamic light scattering, TEM, and AFM for the  $\text{PS}_{200}\text{-}b\text{-P2VP}_{140}\text{-}b\text{-PEO}_{590}$  micelles.<sup>12</sup> However, only a limited reversibility was observed for the  $\text{PS}_{140}\text{-}b\text{-P2VP}_{120}\text{-}b\text{-PEO}_{795}$  micelles.<sup>12</sup> In this work, cylindrical and spherical micelles have been protonated in a 0.1 M HCL aqueous solution. TEM pictures for the protonated micelles are shown in Figure 7, and their geometrical characteristics are listed in Table 3. No pH response is observed, which might be explained by the conformation of the P2VP blocks. Indeed, the thickness of the P2VP shell ( $H_s$ ) for the neutral cylindrical and spherical micelles ( $\text{pH} > 5$ )



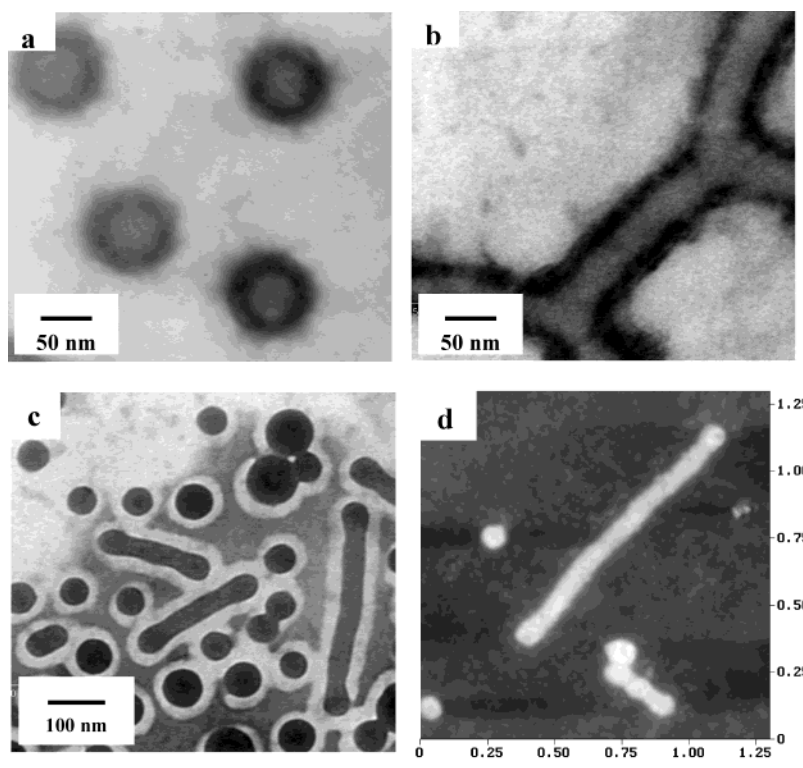


**Figure 4.** Micrographs of PS<sub>200</sub>-*b*-P2VP<sub>140</sub>-*b*-PEO<sub>590</sub> micelles prepared from 70/30 wt/wt DMF-benzene mixture. TEM pictures of micelles contrasted by H<sub>3</sub>PO<sub>4</sub>·12WO<sub>4</sub> (a,b) and thoroughly contrasted by RuO<sub>4</sub> (c); AFM picture of the same micelles (d, height contrast image scaling from 0, black, to 100 nm, white).

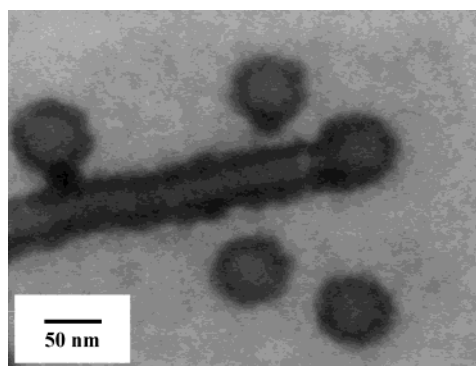


**Figure 5.** TEM micrograph of PS<sub>140</sub>-*b*-P2VP<sub>120</sub>-*b*-PEO<sub>795</sub> micelles prepared from a DMF-benzene (70/30 wt/wt) mixture and contrasted by H<sub>3</sub>PO<sub>4</sub>·12WO<sub>4</sub>.

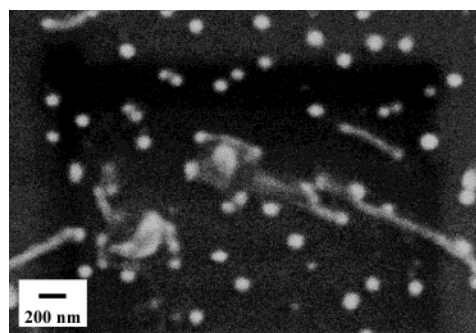


**Figure 6.** SEM image of PS<sub>200</sub>-*b*-P2VP<sub>140</sub>-*b*-PEO<sub>590</sub> micelles (spheres and rods) prepared from a 70/30 wt/wt DMF-benzene mixture.

formed in the presence of benzene (Table 2) is directly comparable to (and certainly not smaller than)  $H_S$  of the spherical micelles at pH < 5 in pure DMF (Table 3). This observation strongly suggests that the P2VP

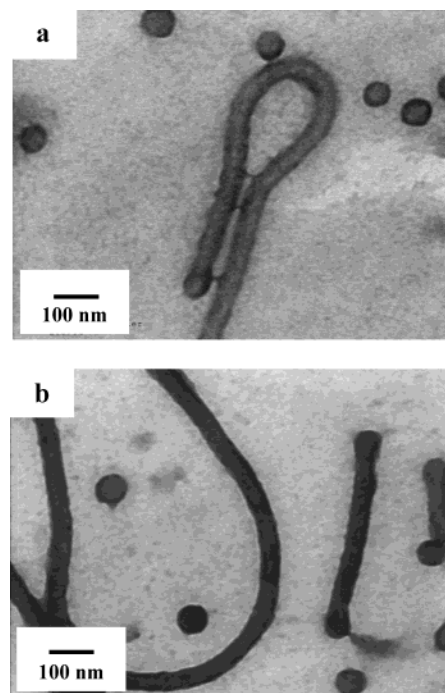


**Figure 7.** TEM micrographs of micelles prepared at pH = 2 from 70/30 wt/wt DMF-benzene mixtures, (a) PS<sub>200</sub>-*b*-P2VP<sub>140</sub>-*b*-PEO<sub>590</sub>, staining with H<sub>3</sub>PO<sub>4</sub>·12WO<sub>4</sub>; (b) PS<sub>140</sub>-*b*-P2VP<sub>120</sub>-*b*-PEO<sub>795</sub>, staining with RuO<sub>4</sub>.

blocks are extended under neutral conditions in micelles formed in the presence of benzene. Therefore, the effect of pH is erased.

To understand the comparative characteristic features for the CSC micelles prepared with and without a solvent selective for the PS block, it must be reminded that the solubility parameter ( $\delta$ ) of benzene [18.8

**Table 3. Shape and Size of the CSC Micelles Formed at pH < 5**

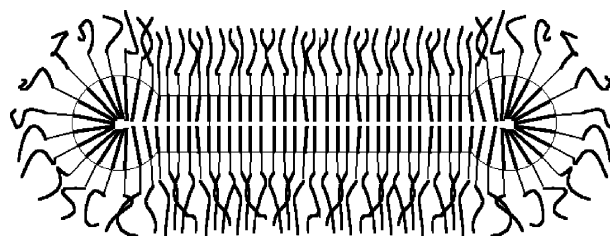
organic solvent	copolymer	morphology	$D_{CS}^a$	$D_C^a$	$H_S^a$
DMF–benzene (70 wt % DMF)	PS <sub>200</sub> – <i>b</i> -P2VP <sub>140</sub> – <i>b</i> -PEO <sub>590</sub>	cylinder	57	28	14
		sphere	74	41	16
	PS <sub>140</sub> – <i>b</i> -P2VP <sub>120</sub> – <i>b</i> -PEO <sub>795</sub>	cylinder	49	26	11
		sphere	62	36	14
DMF <sup>b</sup>	PS <sub>200</sub> – <i>b</i> -P2VP <sub>140</sub> – <i>b</i> -PEO <sub>590</sub>	sphere	50	20	15
	PS <sub>140</sub> – <i>b</i> -P2VP <sub>120</sub> – <i>b</i> -PEO <sub>795</sub>	sphere	31	14	8.5

<sup>a</sup>  $D_{CS}$ ,  $D_C$ ,  $H_S$  and  $H_C$  were extracted from TEM pictures (nm,  $H_C$  is the thickness of the PEO corona). <sup>b</sup> Data for micelles prepared from pure DMF.<sup>12</sup>

(MPa)<sup>1/2</sup>]<sup>18</sup> is much closer to  $\delta$  for PS (16.6–20.2 (MPa)<sup>1/2</sup>) than  $\delta$  for DMF (24.8 (MPa)<sup>1/2</sup>).<sup>16</sup> The PS chains interact thus more strongly with benzene than with DMF. Upon addition of water, the thermodynamic quality of the solvent for the triblock copolymer decreases, and aggregation takes place. This phenomenon has been qualitatively followed by dynamic light scattering by monitoring the scattered intensity as a function of water added to the copolymer solution in a 70/30 wt/wt DMF/benzene mixture. This approach is quite similar to the one previously reported by Eisenberg et al. in order to determine the so-called critical water concentration (CWC) for the formation of crew-cut micelles.<sup>19</sup> Upon addition of a small amount of water, the scattered intensity is very low, in agreement with the persistence of nonaggregated triblock chains. With the addition of approximately 10 wt % of water, the scattered intensity increases importantly, in agreement with micellization. It is referred to as the CWC. At higher water contents, a further dramatic increase in the scattered intensity is observed, which corresponds to the demixing of the ternary solvent mixture.<sup>20</sup> Macroscopically, the system is then similar to an emulsion. At the same time, the benzene-rich phase can accumulate within the PS core of the micelles, whose volume fraction is increased. Conformation and thus entropy of the PS blocks also change. The extent of the PS stretching can be estimated from the ratio of the micellar core radius over the unperturbed end-to-end distance ( $h_0$ ) of PS calculated by eq 1:<sup>21</sup>

$$h_0 = 0.067 M^{1/2} \quad (1)$$

where  $M$  is the molecular weight of the PS block. Clearly, the PS blocks in the cylindrical micelles are stretched compared to the spherical micelles formed from pure DMF (Table 2). Moreover, the stretching of the PS blocks in the spherical micelles formed in the presence of benzene is even higher than in the coexisting cylindrical micelles. These data confirm that the spherical micelles are thermodynamically less stable than the cylindrical ones, which explains how a sphere-to-rod morphological transition is a way to decrease the entropy penalty for the core-forming chains.<sup>15</sup> In this study, the free energy of micellization is accordingly decreased by a sphere-to-rod morphological transition, which is however not complete because the micelles have been frozen out of equilibrium during the dialysis step. Another possible explanation for the incomplete sphere-to-rod transition lies in the polydispersity of the copolymer. In this respect, triblock chains with shorter PS and/or P2VP blocks would accommodate better a spherical morphology. The actual structure of the cylindrical micelles, which is shown in Scheme 1, strongly suggests that the rod-like micelles result from the collapse of benzene-swollen spherical micelles. This statement is supported by the spherical shape of the

**Scheme 1. Schematic Structure of the PS–*b*-P2VP–*b*-PEO Cylindrical Micelles Formed from a DMF–Benzene Mixture**

rod extremities. The stretching of the PS blocks can affect the conformation of the P2VP blocks in the shell, because the chain packing density at the core/shell interface is higher. This effect accounts for the extended conformation of the P2VP blocks at pH > 5. Since the composition of the solvent mixture continuously changes during dialysis, it is impossible to estimate the degree of swelling of the PS core that triggers the rod formation. It may also explain how transient structures, such as onion micelles, can be formed during dialysis. The situation is complicated further by the demixing of the mixture of solvents. At some point, the mobility of the PS chains in the core is strongly decreased as water is substituted for the organic solvents, and the morphology of the micelles is kinetically frozen. Despite the complexity of the rod-like micelle formation, the reproducibility of the experiments must be noted. Indeed, rod-like micelles have been prepared independently under the same conditions, with identical characteristic features and abundance. Finally, benzene (toluene) has been added to spherical triblock micelles in pure water, with formation of an emulsion-like solution. This solution has been dialyzed, and similar rod-like micelles have been collected after dialysis. Nevertheless, no information about the degree of swelling of the PS core of the rod-like micelles can be extracted from this experiment.

In the recent past, steadily increasing attention has been paid to metallic nanoparticles because of their potential in electronic and optical nanodevices.<sup>22</sup> Metallic nanorods and nanotubes are of special interest, for example, in applications in molecular electronics. Metallic nanowires were previously synthesized in rod-shaped templates such as DNA,<sup>23</sup> carbon nanotubes,<sup>24</sup> and brush-like copolymers.<sup>17</sup> Recently, gold nanoparticles were prepared by using PS–*b*-P2VP–*b*-PEO spherical micelles as a template.<sup>11</sup> In this study, PS<sub>200</sub>–*b*-P2VP<sub>140</sub>–*b*-PEO<sub>590</sub> cylindrical micelles have been loaded with AuCl<sub>4</sub><sup>−</sup> ions. Indeed, when the aqueous micellar solution is added with an excess of HAuCl<sub>4</sub>, the gold derivative selectively accumulates and reacts within the P2VP shell. The unreacted HAuCl<sub>4</sub> is removed by dialysis, and the AuCl<sub>4</sub><sup>−</sup> ions are reduced into Au<sup>0</sup> either by the electron beam of TEM or by NaBH<sub>4</sub> or hydrazine. As shown in Figure 8, many gold nanoparticles are

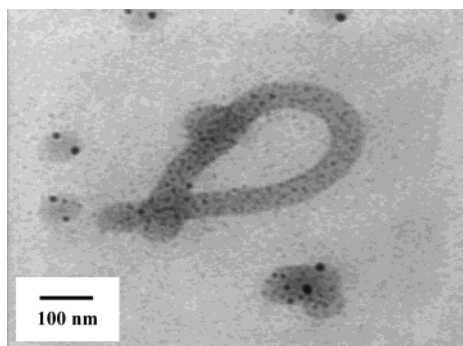


**Figure 8.** TEM image of gold-loaded micelles of PS<sub>200</sub>-*b*-P2VP<sub>140</sub>-*b*-PEO<sub>590</sub> prepared from a 70/30 wt/wt DMF-benzene mixture.

formed in the P2VP shell. AuCl<sub>4</sub><sup>-</sup> loading is, however, not high enough for long-sized nanotubes to be formed. The repeated loading of the micelles is not effective for solving this problem. Metallization of P2VP chains adsorbed on a flat substrate has been recently studied by Minko et al.<sup>25</sup> These authors have shown that metallic rods could be obtained whenever the conformation of the adsorbed P2VP chains is stretched. In sharp contrast, spherical metallic particles are formed in relation to the globular conformation of the P2VP chains. In this work, a globular conformation for the P2VP/AuCl<sub>4</sub><sup>-</sup> complex would prevent continuous gold nanorods from being formed.

## Conclusion

Preliminary dissolution of amphiphilic PS-*b*-P2VP-*b*-PEO triblock copolymers in DMF-benzene (toluene) mixtures (where DMF is a common solvent and benzene a solvent selective for PS) allows cylindrical micelles to be prepared. These cylindrical micelles coexist with spherical ones, from which they originate. Their structure has been analyzed by TEM on the basis of the selective staining of the constitutive subphases. A core-shell-corona three-layer structure is observed with a PS core, a P2VP shell, and a water-soluble PEO corona. AFM and SEM analyses have completed the structural investigation in the dried state. The PS and P2VP blocks are in an extended conformation. Stretching of the PS blocks is thermodynamically unfavorable, which explains that the micellar morphology changes from spheres to cylinders with parallel decrease of the overall free energy of micellization. The cylindrical micelles have been loaded with AuCl<sub>4</sub><sup>-</sup> ions. After reduction, a cylindrical structure with many small gold nanoparticles in the P2VP shell has been observed. The optimization of the experimental conditions in order to form continuous gold nanocylinders rather than isolated nanoparticles is under current investigation.

**Acknowledgment.** J.F.G., "Chargé de Recherches" by the Belgian National Foundation for Scientific Re-

search (F.N.R.S.), thanks the European Science Foundation SUPERNET program. L.L., J.F.G., N.W., and R.J. are very much indebted to the "Services Fédéraux des Affaires Scientifiques, Techniques et Culturelles" for financial support in the frame of the "Pôles d'attraction Interuniversitaires V/03: Supramolecular Chemistry and Supramolecular Catalysis".

## References and Notes

- (1) Hamley, I. W. *The Physics of Block Copolymers*; Oxford University Press: Oxford, 1998.
- (2) Förster, S.; Antonietti, M. *Adv. Mater.* **1998**, *3*, 195.
- (3) Ball, P. *Nature* **2000**, *406*, 118.
- (4) Chang, G. G.; Huang, T. M.; Hung, H. C. *Proc. Natl. Sci. Counc. ROC(B)* **2000**, *24*, 89.
- (5) (a) Chécot, F.; Lecommandoux, S.; Gnagnou, Y.; Klok, H. A. *Angew. Chem., Int. Ed.* **2002**, *41*, 1340. (b) Gohy, J. F.; Varshney, S. K.; Jérôme, R.; *Macromolecules* **2001**, *34*, 3361. (c) Liu, S.; Armes, S. P. *Angew. Chem., Int. Ed.* **2002**, *41*, 1413.
- (6) See for example: (a) Goldacker, T.; Abetz, V.; Stadler, R.; Erukhimovich, I.; Leibler, L. *Nature* **1999**, *398*, 137. (b) Stupp, S. I.; LeBonheur, V.; Walker, K.; Li, L. S.; Huggins, K. E.; Keser, M.; Amstutz, A. *Science* **1997**, *276*, 384.
- (7) (a) Kriz, J.; Masar, B.; Pleštil, J.; Tuzar, Z.; Pospisil, H.; Doskocilova, D.; *Macromolecules* **1998**, *31*, 41. (b) Patrickios, C. S.; Hertler, W. R.; Abbott, N. L.; Hatton, T. A. *Macromolecules* **1994**, *27*, 930. (c) Yu, G.; Eisenberg, A. *Macromolecules* **1998**, *31*, 5546.
- (8) Talingting, M. R.; Munk, P.; Webber, S. E.; Tuzar, Z. *Macromolecules* **1999**, *32*, 1593.
- (9) Erhardt, R.; Böker, A.; Zettl, H.; Kaya, H.; Pyckout-Hintzen, W.; Krausch, G.; Abetz, V.; Müller, A. H. E. *Macromolecules* **2001**, *34*, 1069.
- (10) Liu, S.; Weaver, J. V. M.; Tang, Y.; Billingham, N. C.; Armes, S. P.; Tribe, K. *Macromolecules* **2002**, *35*, 6121.
- (11) Gohy, J. F.; Willet, N.; Varshney, S.; Zhang, J. X.; Jérôme, R. *Angew. Chem., Int. Ed.* **2001**, *40*, 3214.
- (12) Gohy, J.-F.; Willet, N.; Varshney, S. K.; Zhang, J.-X.; Jérôme, R. *e-Polymers* **2002**, *35*.
- (13) Zhang, L.; Eisenberg, A. *Science* **1995**, *268*, 1728.
- (14) (a) Jenekhe, S. A.; Chen, X. L. *Science* **1998**, *279*, 1903. (b) Jenekhe, S. A.; Chen, X. L. *Science* **1999**, *283*, 372.
- (15) Zhang, L.; Eisenberg, A. *Macromolecules* **1999**, *32*, 2239.
- (16) Yu, Y.; Zhang, L.; Eisenberg, A. *Macromolecules* **1998**, *31*, 1144.
- (17) Djalali, R.; Li, S.-Y.; Schmidt, M. *Macromolecules* **2002**, *35*, 4282.
- (18) Lide, D. R. *CRC Handbook of Chemistry and Physics*, 78<sup>th</sup> ed.; CRC press: New York, 1998.
- (19) Zhang, L.; Shen, H.; Eisenberg, A. *Macromolecules* **1997**, *30*, 1001.
- (20) In an initial mixture containing 0.7 g of DMF and 0.3 g of benzene, demixtion is observed whenever a critical amount (0.22 g) of water is added.
- (21) Brandrup, J.; Immergut, E. H. *Polymer Handbook*, 3<sup>rd</sup> ed.; Wiley & Sons: New York, 1989.
- (22) Alivisatos, A. P. *Science* **1996**, *271*, 933.
- (23) Braun, E.; Eichen, Y.; Sivan, U.; Ben-Yoseph, G. *Nature* **1998**, *391*, 775.
- (24) Fullam, S.; Cottell, D.; Rensmo, H.; Fitzmaurice, D. *Adv. Mater.* **2000**, *19*, 1430.
- (25) Minko, S.; Kiriya, A.; Gorodyska, G.; Stamm, M. *J. Am. Chem. Soc.* **2002**, *124*, 10193.

MA034255J